AD-A032 819 NEW YORK UNIV N Y DEPT OF PHYSICS F/G 20/6
MULTIPLE PHOTON IONIZATION PROCESSES IN ATOMS.(U)
JUN 76 E J ROBINSON N00014-67-A-0467-0002
UNCLASSIFIED NL

| OF |
AD
A032819

END
DATE
FILMED
1-77

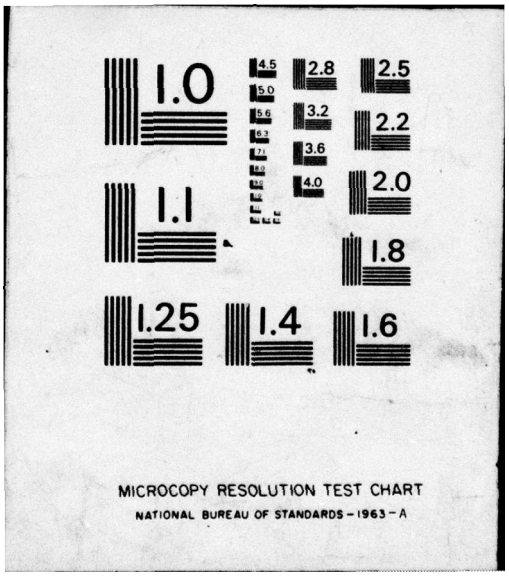
1.0
1.1
1.25
1.4
1.6
1.8
2.0
2.2
2.5
2.8
3.2
3.6
4.0
4.5
5.0
5.6
6.3
7.1
8.0
MICROCOPY RESOLUTION TEST CHART
NATIONAL BUREAU OF STANDARDS - 1963 - A

(18)

(11) Jun 76

(12) 24 p.

AD A032819

(9) FINAL TECHNICAL REPORT,

Contract No. - (15) N00014-67-A-0467-0002

Task No. - NR 014-131X
NR 016-202

Principal Investigator (10) Edward J. Robinson

Source: New York University, Department of Physics
Date: June 1976
Title: Multiple Photon Ionization Processes in Atoms.

(6)

406 850

INTRODUCTION

The advent of the laser has brought about a revolution in the kinds of experimental phenomena that can be investigated. In particular, ultra-high power monochromatic, collimated sources have intensities of sufficient magnitude to enable studies to be carried out in the regime where "non-linear" effects are important, even dominant. Important among these are processes which are characterised by the simultaneous absorption of two or more optical photons. While multiple photon processes are not completely new, (they are, in fact, fairly routine in magnetic resonance work, and known to be the primary mechanism for e^+-e^- annihilation), those in the optical part of the spectrum, like Raman scattering, have, until the advent of the laser, been thought of as linear in the incident intensity, or, like the two-quantum decay of the metastable 2s states of hydrogen-like atoms and ions, been confined to theory.[1] (Recently, of course, these decays have been observed.)

Of the multiple photon, non-linear optical processes, multiquantum ionization is one of the more fruitful for detailed, quantitative measurements, and for comparison with theory, since (1) one does not require precise coincidence between the laser light and an absorption line (2) the ionizations can be detected unambiguously with 100% efficiency (3) atomic wave functions are simple, and (hopefully) sufficiently accurate to enable one to make reasonable precise calculations.

In this project, we produced beams of alkali atoms, cross-fired the atoms with high-intensity electromagnetic radiation, and collected ionization products. While we were prevented by experimental considerations from making absolute measurements of ionization rates (frequency-dependent and intensity-dependent cross-sections), we demonstrated that these ionization rates were a function of the polarization state of the incident radiation[2] (this had not been previously appreciated) and

measured the relative transition probabilities for the different, independent polarization states with sufficient precision to demonstrate that the effect was there and was real, and present some calculations to indicate good agreement between theory and experiment.

Theory

A. Introduction

In reviewing the literature pertaining to multiple quantum transitions in atomic systems one is struck immediately by the absence of any treatment of other than linearly polarized radiation fields. While the treatment of circular polarization does not present any essential difficulties, it would seem that its importance nas been overlooked.

This chapter, then, will serve several purposes. First, it will introduce the higher order perturbation theory appropriate to a treatment of multiphoton transitions. Second, it will briefly review several of the attempts which have been made to solve the resultant equations. Finally, the chapter will indicate the difference which one should expect between the linearly polarized and circularly polarized cases and how this difference might be exploited as a source of polarized electrons.

B. The Perturbation Equation

The transition rate W is expressed by "Fermi's

Golden Rule"

$$W = (2\pi/\hbar)|H'_{fo}|^2\rho(E)$$

where W is the probability of transition per unit time from an initial state ϕ_o to a final state ϕ_f, $\rho(E)$ is the density of the final states and $|H'_{fo}|$ is given by

$$|H'_{fo}| = \sum_j \sum_i \frac{\langle\phi_f|H'|\phi_{N-1}\rangle \cdots\cdots \langle\phi_j|H'|\phi_i\rangle\langle\phi_i|H'|\phi_o\rangle}{[E_i-E_o-\hbar\omega][E_j-E_o-2\hbar\omega]\cdots[E_{N-1}-E_o-(N-1)\hbar\omega]}$$

for a transition of order N with E_o, E_i, E_j and E_f the energies of the initial, the first intermediate, the second intermediate and the final states respectively and ω the frequency of the incident radiation. Assuming the dipole interaction we may write H' as

$$H' = -e\,\underline{E}'\cdot\underline{r}$$

where $\underline{E}'$ is the electric field associated with that part of the incident radiation corresponding to absorption. We can express H' above in terms of the photon flux F by noting that the energy density η can be written in either of two forms:

$$\eta = \frac{(E^2)_{average}}{4\pi} = n\hbar\omega .$$

where n is the number of photons per unit volume and E is the total electric field. Solving this for the amplitude of the electric field and keeping only those terms relating to absorption, we can combine the result with the earlier equations and obtain

$$H'(r) = -\sqrt{2\pi n e^2 \hbar\omega}\ \underline{q}\cdot\underline{r}\ ,$$

where $\underline{q}$ is a unit vector in the direction of polarization and may be considered to stand for either linear or circular polarization at this point. Noting that the photon flux is equal to [n][c] where c is the speed of light and inserting this formula for H' may be inserted into Fermi's Golden Rule to yield

$$|H_{fo}'| = [2\pi R\alpha\hbar^2\omega]^{\frac{1}{2}N}\ (\hbar)^{1-N}\ K_N\ ,$$

where $\alpha = e^2/\hbar c$ is the fine structure constant, N is the order to which the perturbation theory is carried and K_N is defined as

$$K_N = \sum_j \sum_i \frac{\langle\phi_f|\underline{q}\cdot\underline{r}|\phi_{N-1}\rangle \cdots \langle\phi_j|\underline{q}\cdot\underline{r}|\phi_i\rangle\langle\phi_i|\underline{q}\cdot\underline{r}|\phi_o\rangle}{[\omega_{i,o}-\omega][\omega_{j,o}-2\omega]\cdots[\omega_{N-1}-(N-1)\omega]}\ .$$

The $\omega_{k,o}$ frequencies are simply defined as $(E_k-E_o)/\hbar$.

The final states (of momentum $\underline{p}=\hbar\underline{k}$) may be represented by the corresponding ket vectors $|\underline{k}\rangle$ which

obey the orthogonality and closure relations $\langle\underline{k}||\underline{k}'\rangle = (2\pi)^3\delta(\underline{k}-\underline{k}')$ and $\int|\underline{k}\rangle(d\underline{k}/8\pi^3)\langle\underline{k}| = 1$. In the space of $\underline{k}$ vectors, the density of states is, therefore, constant and equal to $(2\pi)^3$. Using the relation $E=p^2/2m$, we obtain the energy density of final states (of energy e):

$$\rho(e) = \frac{(m/\hbar^2)k}{(2\pi)^3}\ .$$

By combining the density of states with the foregoing, we obtain the expression which must be solved:

$$W = \frac{(m/\hbar)[2\pi\alpha F\omega]^N\ k\ |K_N|^2}{(2\pi)^3} = \delta_N F^N\ . \qquad \text{(T-I)}$$

By noting that the ionization potential of the target atoms is greater than twice the energy of a ruby photon, we may begin by considering Eq. (T-I) only for $N \geq 3$.

The expansion parameter upon which the perturbation calculation is based may be represented as the ratio of the radiation field to the coulomb field of the atom. Under the conditions of the experiment 10^8 watts were focused typically into 60 mm^2. The resultant value of the expansion parameter (for these experimental conditions) is approximately 10^{-4}. We may, therefore, specialize Eq. (T-I) to the case of three quantum interactions:

$$W = \delta_3 F^3$$

where δ_3 is defined in Eq. (T-I). The theoretical problem reduces to an evaluation of the infinite summations and a choice of wavefunctions.

C. Average Energy Denominators

Bebb and Gold [3] have generalized Hammerling's [4] method of average energy denominators to solve for δ_3 for hydrogen and the rare gases. Following their notation and assuming light polarized in the z-direction, we find that the rate becomes (for the third order case)

$$K_3 = \sum_{a_1}\sum_{a_2} \frac{\langle a_f|z|a_2\rangle\langle a_2|z|a_1\rangle\langle a_1|z|a_g\rangle}{\{\omega_{1,g}-\omega\}\{\omega_{2,g}-2\omega\}} \qquad \text{(T-II)}$$

where a_g, a_1, a_2, and a_f are the ground, first intermediate, second intermediate and final states respectively. The summations are eliminated by using an "average" frequency $\bar{\omega}(\nu)$ independent of the states. Then Eq. (T-II) may be collapsed to give

$$K_3 = \frac{\langle a_f|z^3|a_g\rangle}{\{\bar{\omega}[1]-\omega\}\{\bar{\omega}[2]-\omega\}} . \qquad \text{(T-III)}$$

One may observe that $\bar{\omega}(\nu)$ is defined by

$$\sum_{a_\nu} \frac{\langle a_f|z^{3-\nu}|a_\nu\rangle\langle a_\nu|z^{\nu}|a_g\rangle}{(\omega_{a_\nu,a_g}-\nu\omega)} = \frac{\langle a_f|z^3|a_g\rangle}{(\bar{\omega}[\nu]-\nu\omega)} . \qquad \text{(T-IV)}$$

This result is obtained by defining $\bar{\omega}(\nu)$ in each successive order ν by equating the right hand sides of Eqs. (T-II) and (T-III). Additional reduction is made possible by assuming that there exists a single "average" frequency for the virtual states $\bar{\omega}_\nu$ independent of the order ν. This new average frequency is

$$\prod_{\nu=1}^{\nu=2}\{\bar{\omega}(\nu)-\nu\omega\} = \prod_{\nu=1}^{\nu=2}\{\bar{\omega}_\nu-\nu\omega\} . \qquad \text{(T-V)}$$

The third order matrix element then becomes

$$K_3 = \frac{\langle a_f|z^3|a_g\rangle}{(\bar{\omega}_\nu-\omega)(\bar{\omega}_\nu-2\omega)} . \qquad \text{(T-VI)}$$

In this form the problem of evaluating K_3 becomes one of determining the "average frequency" which is, in principle, well defined by Eqs. (T-V) and (T-VI). Bebb and Gold make use of the existance of "near resonances" in the excitation spectrum to determine those states which make dominant contributions to $\bar{\omega}_\nu$. The hydrogenic wavefunctions used by Bebb and Gold are also applicable to cesium. In the next section, however, a more accurate procedure used by Bebb to solve for δ_3 is described.

D. Explicit Summation

Bebb [5] explicitly performs the summations in Eq (T-II) without resort to the average frequency approach. He proceeds by

using the quantum-defect method for matrix elements. These are calculated with coulomb functions whose principal quantum number is adjusted to conform to the observed energy levels of the atom in question. The effective quantum number υ_ℓ is defined by $I_{n\ell}=Z^2/\upsilon_\ell$ where $I_{n\ell}$ is the energy in Rydbergs and Z is the residual charge on the ion. The quantum defect is then simply υ_ℓ-n. This adjustment results in radial wavefunctions $R_\ell(k,r)$ which asymptotically approach

$$R_\ell(k,r) \underset{kr\longrightarrow\infty}{\approx} [kr]^{-1}\sin(x + \xi(k^2)) \quad \text{(T-VII)}$$

where

$$x = kr + [k]^{-1}\ln[2kr] - \tfrac{1}{2}\ell\pi + \eta_\ell \quad \text{(T-VIII)}$$

This $\xi(k^2)$ is the "quantum defect" and can be analytically continued beyond the ionization potential.

Bebb writes the integrated transition probability in terms of an "ionization strength" given by

$$W_{k,g} = 2\pi\hbar\{2\pi\alpha F\omega\}^3\, S^{(3)}(k;g) \quad \text{(T-IX)}$$

where

$$S^{(3)}(k;g) = \frac{\rho(E_{fin})}{g_o}\sum_m \int d\Omega_k |\langle \underline{k}|T^{(3)}|g\rangle|^2 \quad \text{(T-X)}$$

In Eq. (T-X) the ground state is denoted by g and the continuum states are specified by the electron propagation vector $\underline{k}$. The degeneracy of the ground state is g_o and $T^{(3)}$ is given by

$$T^{(3)} = \left\{\prod_{\nu=1}^{\nu=2}\sum_{a_\nu}\frac{z|a_\nu\rangle\langle a_\nu|}{(\omega_{a_\nu,g}-\nu\omega)}\right\} z \quad \text{(T-XI)}$$

One notices in Eq. (T-VI) that, once again, the assumption of linearly polarized incident radiation has been introduced. As indicated above, Bebb takes as final state wavefunctions the expression

$$|k\rangle = 4\pi\sum_{m_s}\sum_{m_\ell}\sum_{\ell}\left[\, i^\ell e^{i\eta_\ell}\, Y_\ell^{m\ell *}(\theta,\phi)\, |k,\ell,m_\ell,m_s\rangle\right] \quad \text{(T-XII)}$$

where

$$|k,\ell,m_\ell,m_s\rangle = R_\ell(k;r)Y_\ell^{m\ell}(\theta,\phi)\,\chi(m_s)\ , \quad \text{(T-XIII)}$$

and where R(k;r) is given in Eq. (VII). By restricting attention to one-electron atoms with s ground states, incorporating selection rules appropriate to dipolar matrix elements and using Clebsh-Gordan coefficients to express $S^{(3)}$ in terms of elements involving m_ℓ, m_s functions, Bebb obtains the result

$$S^{(3)}(k;n,s,\tfrac{1}{2}) = \rho(E_{fin})(4\pi)^2 \sum_{m=-j}^{m=+j} \sum_{s',m_s'}$$

$$\Big| \sum_{[ns]_2} \sum_{[ns]_1} \sum_{\nu=-\frac{1}{2}}^{\nu=+\frac{1}{2}} \Big[\langle s_2,\tfrac{1}{2},m-m_s'|J_2,m\rangle$$

$$\langle s_2,\tfrac{1}{2},m-\nu,\nu|J_2,m\rangle \langle p,\tfrac{1}{2},m-\nu,\nu|J_1,m\rangle \Big]$$

$$\langle p,\tfrac{1}{2},0,\tfrac{1}{2}|J_1,m\rangle \langle k,s',m-m_s'|z|[ns]_2,m-m_s'\rangle$$

$$\frac{\langle [ns]_2,m-\nu|z|[np]_1,m-\nu\rangle \langle [np]_1,0|z|ns_{\frac{1}{2}}0\rangle \Big|^2}{\Omega(ns)_2\,\Omega(np)_1} \qquad \text{(I-XIII)}$$

where the energy denominators are defined by

$$\hbar\Omega(ns)_\sigma = E(n_\sigma s_\sigma J_\sigma) - E(ns) - \sigma\hbar\omega \,. \qquad \text{(I-XIV)}$$

In Eq. (I-XIV) the summation over first-order intermediate states is dominated by the lowest lying configuration due simultaneously to the large value of the corresponding matrix element and the occurance of a near resonance of the photon energy (for all frequencies ≤ I/3) with the (n_g,p) configuration. The sum over the second-order s and d states is well approximated by keeping only the near resonant terms indicated in Fig. 1. The figure represents the results of Bebbs's calculations, plotted on a Calcomp digital plotter driven by an IBM 7074 computer. We observe that, for radiation at the ruby-laser frequency, Bebb's method gives the result

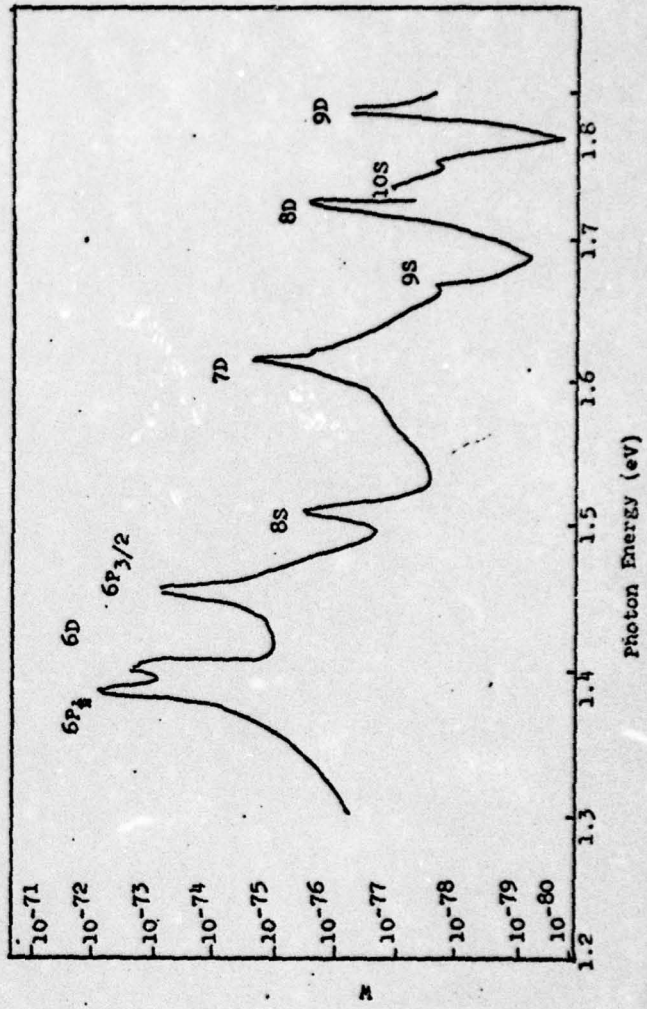

Figure 1

$$\delta_3 = 6 \times 10^{-78}\ \text{cm}^6\text{-sec}^2$$

for linearly polarized incident radiation.

E. Implicit Summation

In general, the method of implicit summation consists of the replacement of sums of matrix elements with a single element between the initial or the final state and a state obtained from a solution of one or more inhomogenous Schrodinger's equations. Robinson * applied a form of this technique to the case in question using a numerical form of the atomic potential and the unperturbed cesium wavefunctions. With the definitions

$$|M_1\rangle = \Sigma \frac{|j\rangle\langle j|z|f\rangle}{(\omega_{j,o}-2\omega)} \qquad \text{(T-XVI)}$$

and

$$|M_2\rangle = \Sigma \frac{|k\rangle\langle k|z|g\rangle}{(\omega_{k,o}-\omega)} \qquad \text{(T-XVII)}$$

becomes

$$K_3 = \langle M_2|z|M_1\rangle \qquad \text{(T-XVIII)}$$

$|M_1\rangle$ and $|M_2\rangle$ satisfy the equations

*The calculation is discussed in detail in a later section.

$$(H_o-E_o-2\hbar\omega)|M_1\rangle = z|f\rangle \qquad \text{(T-XIXa)}$$

$$(H_o-E_o-\hbar\omega)|M_2\rangle = z|g\rangle. \qquad \text{(T-XIXb)}$$

To outline the method we may confine ourselves to the solution of Eq. (XIX-b). We will employ atomic units in which $e=\hbar=m_e=a_o=1$. By evaluating the angular part of $|M_2\rangle$ immediately and employing the explicit form of H_o we can write

$$\left[(-d^2/dr^2)-(2/r)(d/dr)+(2/r^2) \right.$$
$$\left. -(2/r)+\alpha^2-\omega \right] u_1(r) = r u_o(r) \qquad \text{(T-XIX-c)}$$

where u(r) is the radial part of $|M_2\rangle$, α^2 is the electron energy and where use has been made of the following asymptotic forms of the atomic potential and the unperturbed wavefunction:

for large r:

$$V(r) \approx -1/r$$

$$u(r) \approx r^s \exp(-\alpha r) \sum_k a_k r^{-k}. \qquad \text{(T-XX)}$$

In Eq. (T-XX) s is a non-integer "effective quantum number" similar to υ_ℓ as defined in section D of this chapter. Solution of Eq.(XIX-c) is accomplished by

expressing $u_1(r)$ in the form $F(r)\exp(-\alpha r)$. Once this asymptotic form of $u_1(r)$ has been found Eq. (XIX-a) is transformed from a differential equation to a finite difference equation which is solved numerically. The results of this implicit solution as applied to a one-electron atomic model (for the cesium atom in linearly polarized radiation at the ruby-laser frequency) are:

$$\delta_3 = 3 \times 10^{-77} \text{ cm}^6\text{-sec}^2.$$

F. Polarization Effects

As has been previously indicated, we have been unable to find previous discussions of circularly polarized light and multiple quantum processes. It is possible that circularly polarized light was ignored because of the natural, but erroneous, assumption that the unpolarized nature of the atomic systems would cause the transition probabilities to be independent of the polarization of the incident radiation. Indeed, it is true that transition rates for unpolarized targets interacting with either member of an orthogonally polarized pair will be the same.

This experiment is the first to present evidence contrary to this assumption. As we shall show in a later section, there is a distinct difference in the transition probabilities under the influence of circularly, as compared to linearly, polarized light. It is the purpose

of this section to discuss qualitatively why this is so. In addition, we indicate the possibility that such differences can be exploited as a source of polarized electrons.

Fig. 2 represents those virtual states of the cesium atom (treated as a single active electron with an inert core) which are accessable to an electron, initially in the ground state, which absorbs three successive linearly polarized photons. The appropriate selection rules are then

$$\begin{aligned} \Delta\ell &= \pm 1 \\ \Delta j &= \pm 1, 0 \\ \Delta m &= 0 \ . \end{aligned} \qquad \text{(T-XXI)}$$

The notation used to indicate energy levels in the figure is

$$^{2s+1}\ell_j(m_j). \qquad \text{(T-XXII)}$$

Each level in the figure represents the infinite set of levels which have angular momentum quantum numbers as given by Eq. (XXII). Those states whose m_j values render them inaccessable from the initial $m_j=+\frac{1}{2}$ have been omitted. In addition, the transitions starting from the the $m_j=-\frac{1}{2}$ have also been omitted for clarity. (They may

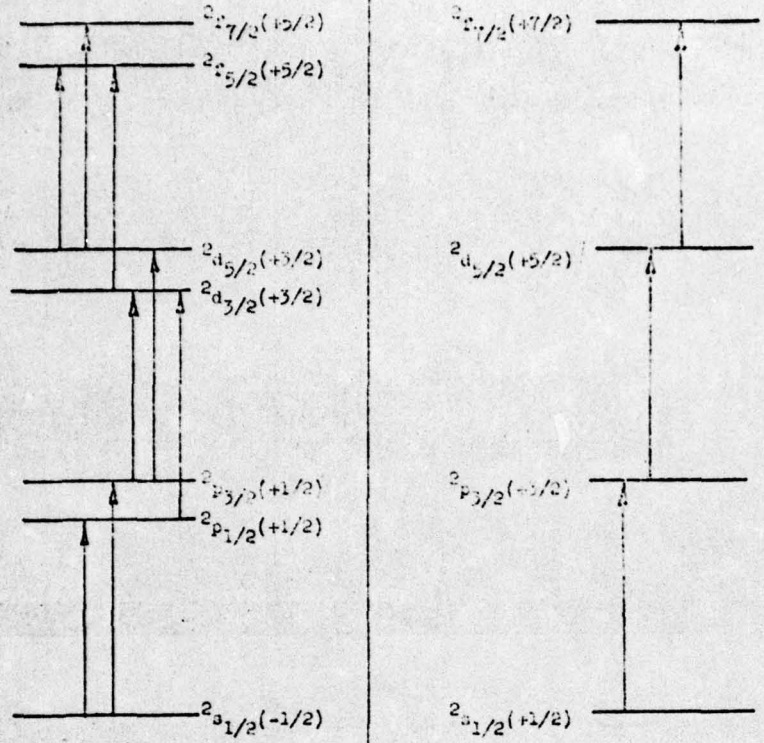

Figure 3

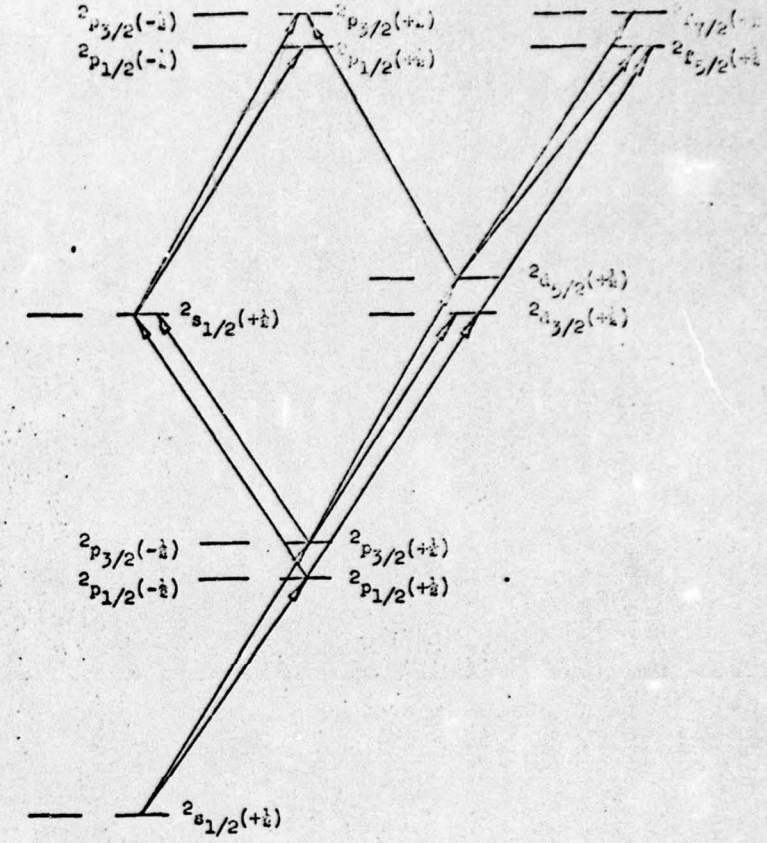

Figure 2

be obtained by interchanging + and - signs on all m_j values).

Fig. 3 considers the transition channels open under the influence of right circularly polarized light propagating along the reference axis. Under these circumstances the selection rule is $\Delta m_j = +1$. Since the open transition channels are different for the $m_j = +\frac{1}{2}$ ground state and the $m_j = -\frac{1}{2}$ ground state, they are exhibited separately. The difference in the number and the character of the open transition channels between Figs. 2 and 3 is striking. One should note in passing that the effect of the right circularly polarized light on the $m = -\frac{1}{2}$ and the $m = +\frac{1}{2}$ ground states is identical with the effect of left circularly polarized light on the $m = +\frac{1}{2}$ and $m = -\frac{1}{2}$ ground states respectively. Thus, for an unpolarized target beam such as ours, we find no difference in the transition rates when the "sense" of the polarization is reversed.

A quantitative comparison of the linearly and circularly polarized cases awaits the evaluation of the appropriate matrix element sums. Briefly, the procedure would be to define a second ionization strength for circularly polarized light similar to the one in Eq. (T-IX). By explicitly writing the individual terms in the summations of Eq. (T-IX) and its analog and applying the Wigner-Eckart theorem both ionization strengths could be expressed as sums of matrix

elements of the form

$$\langle n'\ell'_{j'}|r|n\ell_j\rangle$$

thereby permitting comparison.

A comparison involving significantly less computation may be made by ignoring the effect of spin. Such a comparison serves the dual purpose of illustrating that the effect is not dependent upon spin-orbit coupling and providing a model for calculation in the more complicated case.

In this approximation Eq. (T-IX) reduces to

$$S^{(3)} = (\rho)(4\pi)^2 \Big[\Big| \sum\sum_{nn'} \frac{1}{\Omega(n's)\Omega(np)} \langle kp0|z|n's0\rangle \cdot \langle n's0|z|np0\rangle\langle np0|z|n_g s0\rangle + \sum\sum_{nn'} \frac{1}{\Omega(n'd)\Omega(np)} \langle kp0|z|n'd0\rangle\langle n'd0|z|np0\rangle\langle np0|z|n_g s0\rangle \Big|^2 + \Big| \sum\sum_{nn'} \frac{1}{\Omega(n'd)\Omega(np)} \langle kf0|z|n'd0\rangle \langle n'd0|z|np0\rangle\langle np0|z|n_g s0\rangle \Big|^2 \Big] \quad \text{(T-XXIII)}$$

and $C^{(3)}$ (the ionization strength for circularly polarized light) becomes

$$C^{(3)} = (\rho)(4\pi)^2 \left| \sum_{nn'} \frac{1}{\Omega(n'd)\Omega(np)} \langle kf3|\frac{x+iy}{\sqrt{2}}|n'd2\rangle \right.$$

$$\left. \langle n'd2|\frac{x+iy}{\sqrt{2}}|np1\rangle\langle np1|\frac{x+iy}{\sqrt{2}}|n_g s0\rangle \right|^2 \qquad \text{(T-XXIV)}$$

Applying the Wigner-Eckart theorem to Eqs.(XXIII) and (XXIV) and dividing, we obtain:

$$C^{(3)}/S^{(3)} = \frac{2.5|C|^2}{|C|^2 + (1/90)|A+4B|^2}, \qquad \text{(T-XXV)}$$

where

$$A = \sum_{nn'} \frac{1}{\Omega(n's)\Omega(np)} \langle kp\| r\| n's\rangle\langle n's\| r\| np\rangle\langle np\| r\| n_g s\rangle$$

$$B = \sum_{nn'} \frac{1}{\Omega(n'd)\Omega(np)} \langle kp\| r\| n'd\rangle\langle n'd\| r\| np\rangle\langle np\| r\| n_g s\rangle$$

$$C = \sum_{nn'} \frac{1}{\Omega(n'd)\Omega(np)} \langle kf\| r\| n'd\rangle\langle n'd\| r\| np\rangle\langle np\| r\| n_g s\rangle .$$

(T-XXVI)

G. A Polarized Electron Source

The use of this effect as a source of polarized electrons is suggested by examination of the difference in open transition channels between the left and the right sides of Fig. 3. The operative principle is that polarization is transferred to the target atoms during virtual transitions. After the absorption of the first

photon, the interaction takes place between a polarized atom and successive polarized photons. Each successive absorption increases the degree of polarization of the target.

In a procedure similar to the one followed in the last section, we can define ionization strengths C_+ and C_- for the effect of right circularly polarized light incident on an atom in the $m=+\frac{1}{2}$ and $m=-\frac{1}{2}$ ground states respectively. If $q=x+iy$:

$$C_- = (5/48)\left| \sum_{nn'} \frac{1}{\Omega(n'd_{3/2})\Omega(np_{\frac{1}{2}})} \langle kf|q|n'd_{3/2}\rangle\langle n'd_{3/2}|q|np_{\frac{1}{2}}\rangle \right.$$

$$\langle np_{\frac{1}{2}}|q|n_g s_{\frac{1}{2}}\rangle + \sum_{nn'} \frac{1}{\Omega(n'd_{3/2})\Omega(np_{3/2})} \langle kf|q|n'd_{3/2}\rangle$$

$$\langle n'd_{3/2}|q|np_{3/2}\rangle\langle np_{3/2}|q|n_g s_{\frac{1}{2}}\rangle + \sum_{nn'} \frac{1}{\Omega(n'd_{5/2})\Omega(np_{3/2})}$$

$$\left. \langle kf|q|n'd_{5/2}\rangle\langle n'd_{5/2}|q|np_{3/2}\rangle\langle np_{3/2}|q|n_g s_{\frac{1}{2}}\rangle \right|^2$$

$$+ (81/160)\left| \sum_{nn'} \frac{1}{\Omega(n'd_{5/2})\Omega(np_{3/2})} \langle kf|q|n'd_{5/2}\rangle \right.$$

$$\left. \langle n'd_{5/2}|q|np_{3/2}\rangle\langle np_{3/2}|q|n_g s_{\frac{1}{2}}\rangle \right|^2 \qquad \text{(T-XXVII)}$$

and

$$C_+ = (45/16)\left| \sum_{nn'} \frac{1}{\Omega(n'd_{5/2})\Omega(np_{3/2})} \langle kf|q|n'd_{5/2}\rangle \right.$$

$$\left. \langle n'd_{5/2}|q|np_{3/2}\rangle\langle np_{3/2}|q|n_g s_{\frac{1}{2}}\rangle \right|^2 .$$

(T-XXVIII)

For ease of comparison we can redefine C_+ and C_- as

$$C_+=(45/16)\ |A|^2$$

$$C_-=(5/48)\ |B+C+A|^2 + (81/160)\ |A|^2. \quad \text{(T-XXIX)}$$

Dividing C_- by C_+ we obtain

$$C_-/C_+ = (1/27)\ |\ 1 + (B/A) + (C/A)\ |^2 + (9/50)\ . \quad \text{(T-XXX)}$$

By a proper choice of frequencies, the terms involving $\Omega(np_{3/2})$ can be made to dominate over the terms involving $\Omega(np_{\frac{1}{2}})$. For example, in the case of cesium, the $7p_{3/2}$ and the $7p_{1/2}$ states lie 4594.39 Å and 4556.50 Å above the ground state respectively.[27] This corresponds to a frequency difference of 543×10^{10} Hz. Incident light of the appropriate frequency can, by this process, selectively photoionize atoms and, thereby, produce polarized electrons.

Chapter IV: The Experimental Technique

A. Introduction

Under "Theory," it was shown that, in the realm to which perturbation theory applies, the photoionization probability per atom and per unit time is proportional to F^n where F is the incident photon flux (in photons/cm^2-sec) and where n is the order to which the perturbation theory is carried out. It is the purpose of this chapter to show that the value of the coefficient of proportionality in the third order (δ_3) can be obtained by measuring the incident light flux, the incident atomic current, the temperature of the atomic beam, the number of photoionized atoms and the interaction geometry.

B. Calculation of the Coefficient

The calculation is based on the interaction geometry depicted in Fig. 4. The diameter of the laser spot is given by d and the height and width of the atomic beam by h_{int} and ℓ_{int} respectively. The number N of atoms which will be photoionized is given by

$$N = \int \rho\ W\ dt\ dV \qquad \text{(E-I)}$$

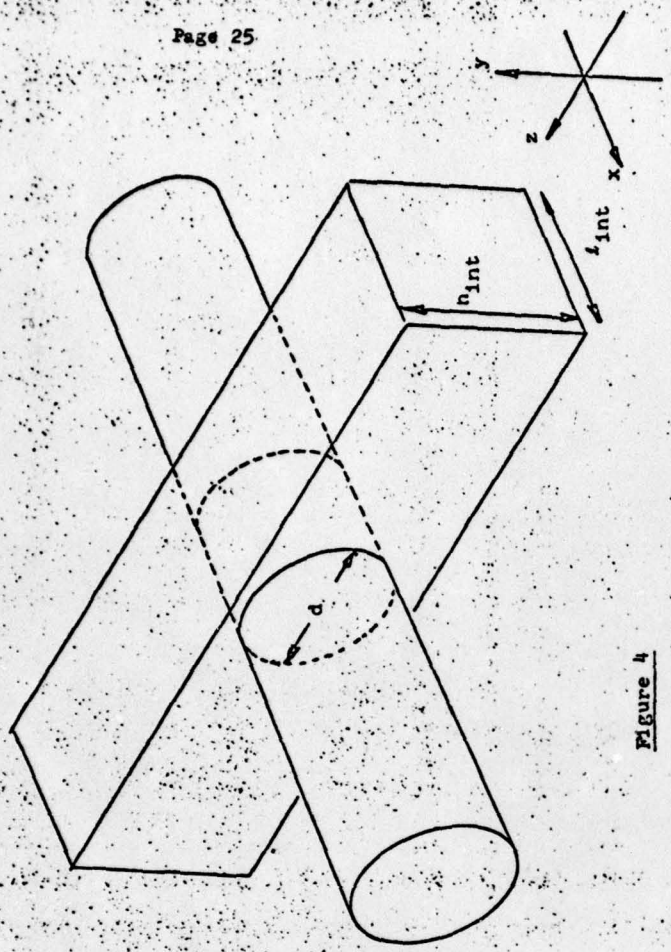

Figure 4

where W is the photoionization probability per atom and per unit time, ρ is the density of atoms in the interaction region, V is the volume of intersection of the laser and atomic beams, and where the time integral is performed over the period during which the laser is on.

If only a small fraction of the atoms in the beam are photoionized during the time that the laser is on, ρ may be considered constant and removed from the time integral. As was mentioned earlier, the incident laser flux was typically 10^8 watts into 0.6 cm^2 for a period of approximately 20 nsec. Using these values and the largest estimate for σ_3 results in the estimate that only 0.01% of the atoms are photoionized. Under these circumstances, then, we consider ρ constant.

The photoionization probability W (as presented in "Theory") is given by

$$W = \sigma_3 \overline{F^3(y,z)} \; . \qquad \text{(E-II)}$$

(The bar over the flux is used to emphasize that the observed flux is averaged over many periods of the laser oscillation but over a time short compared to the width of the laser pulse.). The atom density is given by

$$\rho = \frac{J(x,y)}{\langle v \rangle} \qquad \text{(E-III)}$$

where J(x,y) is the atomic current density and <v> is the average speed of an atom in the beam. Combining Eqs. (E-II) and (E-III) with Eq. (E-I), and introducing the assumption that J(x,y) is constant within the interaction volume, one obtains

$$N = \frac{J(x,y)\delta_3 \ell_{int}}{\langle v \rangle} \int \overline{P^3}(y,z)\, dA dt, \qquad \text{(E-IV)}$$

where A is the area of the laser spot as it intersects the atomic beam.

$\overline{P^3}$ may be replaced by $3!P^3$ where 3! is a temporal coherence correction resulting from the simultaneous oscillation of different laser modes. The result is

$$N = \frac{J(x,y)\delta_3 \ell_{int}\{\pi d^2/4\}(6)}{\langle v \rangle} \iint P^3 dt\, dA. \qquad \text{(E-V)}$$

By inverting Eq. (E-V) we obtain our initial expression for δ_3 in terms of the experimental parameters

$$\delta_3 = \frac{N\langle v \rangle}{6J(x,y)\ell_{int}\{\pi d^2/4\}\iint P^3 dt\, dA}. \qquad \text{(E-VI)}$$

C. Average Velocity of the Atoms

Since the atomic beam source is a vapor in equilibrium with the walls of an alkali oven, the number density velocity distribution n(v) is given by the Maxwell-Boltzmann expression

$$n(v) = Cv^2 \exp(-\tfrac{1}{2}\mu v^2/kT) \qquad \text{(E-VII)}$$

where C is (for these purposes) a constant, v is the atomic velocity, μ is the atomc mass, k is Boltzmann's constant and T is the absolute temperature of the vapor. The average velocity is, then,

$$\langle v \rangle = \frac{\int_0^\infty vn(v)\, dv}{\int_0^\infty n(v)\, dv} = (8kT/\mu\pi)^{\frac{1}{2}}. \qquad \text{(E-VIII)}$$

The average atomic velocity may, therefore, be written as

$$\langle v \rangle = 1.449 \times 10^4 (T/M)^{\frac{1}{2}} \text{ cm/sec} \qquad \text{(E-IX)}$$

where M is the mass of the atom in a.m.u..

D. The Laser Spot Size

The laser spot size d is not measured directly but is obtained from the relationship

$$d = [\theta][\Gamma], \qquad \text{(E-X)}$$

where θ is the divergence of the laser beam and Γ is the focal length of the lens used to focus the laser beam (originally 9/16 in. in diameter) down to the spot diameter. Eq. (E-X) is readily justified by reference to Fig. 5. The phenomenon of beam

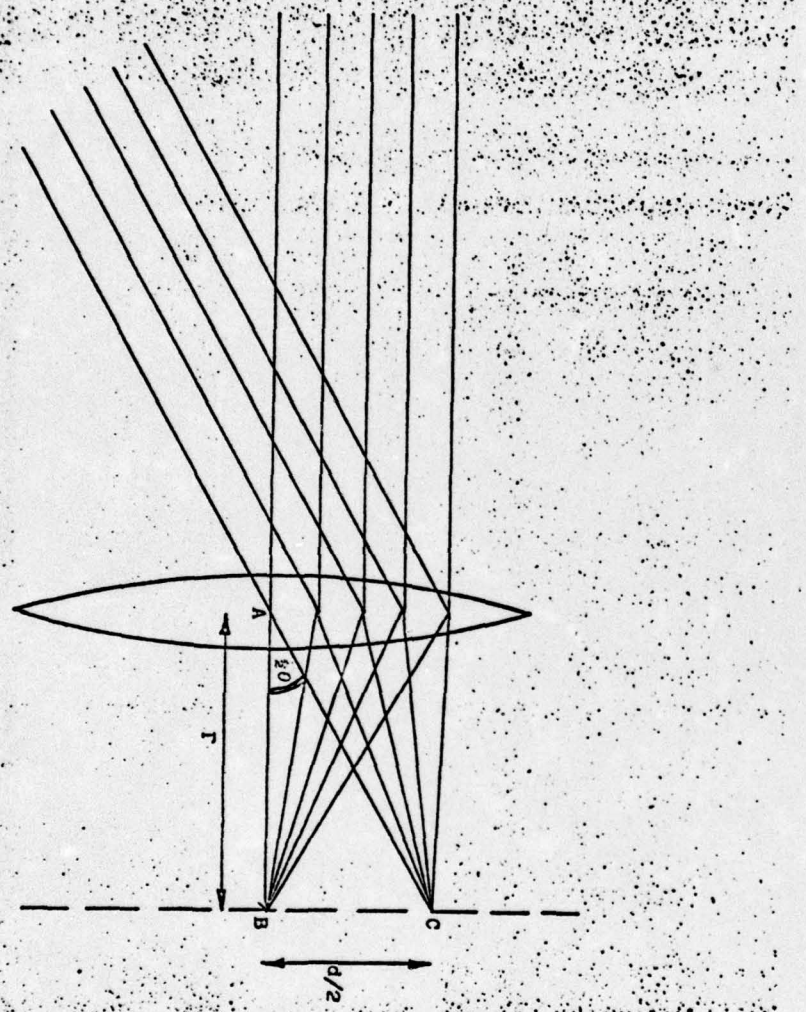

Figure 5

divergence has its source in the fact that the light rays are emanating from a variety of points within the laser rod and are propagating at a variety of angles with respect to the optical axis. As indicated in Fig. 5 those rays which are propagated parallel to the optical axis are focused to a point on the axis at a distance from the principal plane of the lens equal to its focal length. A group of rays hitting the lens at an angle ½θ from the axis is focused to a point in the same focal plane but at a distance d/2 from the axis. One observes that, since those rays which pass through the center of the lens are undeflected, triangle ABC is a right triangle with AB = Γ and BC = d/2 and angle CAB = θ/2. If θ/2 represents half the beam divergence angle then d/2 represents the radius of the minimum spot size into which the beam may be focused. For small angles (in our case θ is on the order of milliradians)

$$\tfrac{1}{2}d = [\Gamma][\tan\{\tfrac{1}{2}\theta\}] \approx [\Gamma][\tfrac{1}{2}\theta] \qquad \text{(E-XI)}$$

E. Determination of the Beam Current

1. Effective Height of the Detector

J(x,y) as it appears in Eq. (E-III) represents the number of atoms per second which pass across a unit area perpendicular to the atomic beam axis and located at the point of the interaction. This parameter may be indirectly measured by a beam profile

analysis combined with a knowledge of the appropriate beam dimensions. Fig. 6 displays the relative positions and sizes of the oven exit slit, the beam collimating slit and the hot-wire detector. The presence of the collimating slit gives rise to an atomic beam whose intensity as a function of the distance off-axis is trapezoidal in shape. Fig. 7 shows this function as it would be measured by an ideal (zero width) detector and as it would be measured by a detector of finite width.

In view of the intensity fall-off in the penumbra, an "effective detector height" must be defined to adjust for the uneven contributions to the detector current made by that part of the detector height within the umbra and that part which is in the penumbra. If, as in Fig. 6, one defines H to be the height of the umbra, H' to be the height of the umbra-plus-penumbra and h to be the height of the detector then

$$h_{eff} = H + (h + H' - 2H)(h - H)/(2H' - 2H). \qquad \text{(E-XII)}$$

It should be noted that the values given in Fig. 6 for the beam umbra and penumbra are obtained by direct calculation from the known values of the beam geometry. The values used in the calculations presented in this section are, instead, those obtained from measurements of the atomic beam profile.

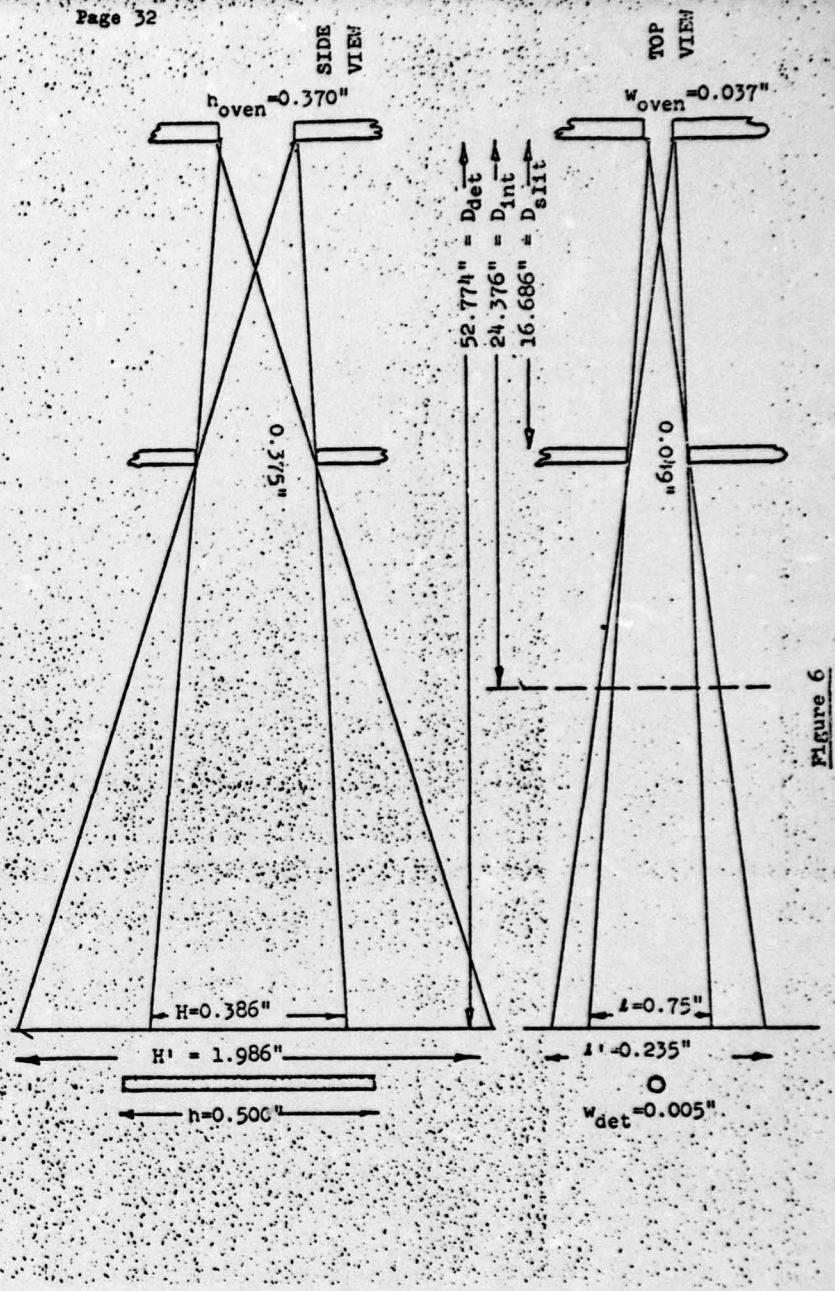

Figure 6

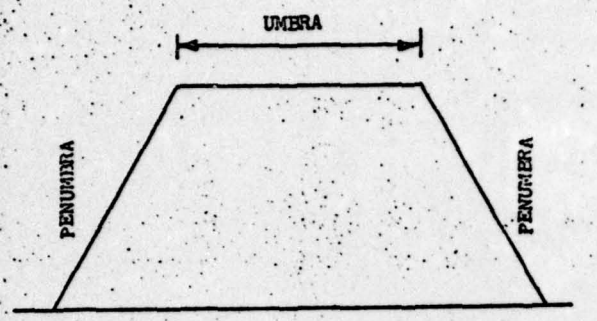

(a)

(b)

Figure 7

Although at large atomic beam current there is appreciable broadening, the profile parameters were stable over the range of currents obtained during the data-taking. In this range the full width of the umbra ℓ was found to be 44.0 mils and the full width of the base of the profile trapezoid ℓ' was found to be 224.0 mils. Inserting these values for the parameters into Eq.(E-XII) we obtain

$$h_{eff} = 0.441 \text{ in} = 11.201 \text{ mm}. \qquad \text{(E-XIII)}$$

2. Mapping the Beam Profile

Since the laser passes through the entire width of the atomic beam, it is necessary to determine how the current density behaves as a function of x (see Fig. 4 for a definition of x). This is done by translating the hot-wire detector along the x-direction and then "mapping backwards" to the interaction region. By the use of similar triangles, one may readily verify that

$$(\ell_{int}-w_{oven})/(\ell-w_{oven}) = \alpha \qquad \text{(E-XIV)}$$

$$(\ell'_{int}+w_{oven})/(\ell'+w_{oven}) = \alpha \qquad \text{(E-XV)}$$

$$(h_{int}-h_{oven})/(h_{eff}+h_{oven}) = \alpha \qquad \text{(E-XVI)}$$

where ℓ, ℓ', h_{oven} and w_{oven} are defined in Fig 6,

α is defined as D_{int}/D_{det} and is equal to 0.461 in and ℓ_{int}, ℓ'_{int}, and h_{int} are the interaction region analogs of ℓ, ℓ', and h_{eff} respectively.

Inserting the actual parameters of the apparatus into Eq.(E-XIV) and (E-XV),one obtains

$$\ell_{int} = 0.040 \text{ in} = 1.016 \text{ mm} \qquad \text{(E-XVII)}$$

$$\ell'_{int} = 0.083 \text{ in} = 2.108 \text{ mm.} \qquad \text{(E-XVIII)}$$

In a manner similar to that used in Section III E 1, we define the effective interaction region beam width ℓ_{eff} to be

$$\ell_{eff} = \ell_{int} + \tfrac{1}{2}(\ell'_{int}-\ell_{int})$$

$$= \tfrac{1}{2}(\ell'_{int} + \ell_{int})$$

$$= 0.062 \text{ in} = 1.575 \text{ mm} \qquad \text{(E-XIX)}$$

3. Mapping the Current Density

If I_o is the atomic beam current (in amps) in the umbra of the beam as read by a detector of height h_{eff} and width w_{det}, then the current density in the umbra is

$$J_o = I_o/(h_{eff}w_{det}) \qquad \text{(E-XX)}$$

Taking into account the loss of beam intensity in the penumbra, we find that the total number of atoms which pass the detector plane to a height h_{eff} in each second is

$$(I_o/w_{det})(\ell + \tfrac{1}{2}\{\ell'-\ell\}) = (I_o/2w_{det})(\ell'+\ell). \qquad \text{(E-XXI)}$$

This same number of particles passes an analog area in the interaction region which is given by $A_{int}=\ell_{eff}h_{int}$. With the use of Eqs. (E-XII),(E-XIV),(E-XV), (E-XVI), and (E-XIX), we can write

$$A_{int} = (\alpha h_{eff}+[1-\alpha]h_{oven})(\tfrac{1}{2}\alpha\{\ell+\ell'\}). \qquad \text{(E-XXII)}$$

Using Eqs. (XXI) and (XXII), we can write the current density in the interaction region as

$$J_{int}(x,y) = \frac{I_o}{w_{det}(\alpha^2\{h_{eff}-h_{oven}\}+\alpha h_{oven})}. \qquad \text{(E-XXIII)}$$

Inserting the experimental parameters for w_{det}, h_{eff}, h_{oven} and α we obtain

$$J_{int}(x,y) = 6.25 \times 10^{21} I_o \text{ (part/sec-in}^2\text{)} \qquad \text{(E-XXIV)}$$

$$= 0.97 \times 10^{21} I_o \text{ (part/sec-cm}^2\text{).}$$

F. Relationship Between Laser Flux and Laser Power

The spatial average flux $\langle F \rangle$ which appears implicitly in Eq. (E-VI) is expressed in units of photons/cm^2-sec. Physically what takes place is that the full power of the laser is focused down so that it intersects the atomic beam in a spot of diameter d (see Eq. (E-X)). The average flux is indirectly measured by monitoring the laser power and dividing it by the area into which the laser is focused. If P is the instantaneous power of the incident light (in watts) and if $\hbar\omega$ is the energy contained in a single photon, then

$$\langle F \rangle = \frac{(P/\hbar\omega)}{\pi(d/2)^2} \text{ photons/cm}^2\text{-sec.} \quad \text{(E-XXV)}$$

Combining Eqs. (E-X) and (E-XXV), we may write $\langle F \rangle$ as

$$\langle F \rangle = \frac{P}{\omega\theta^2\Gamma^2} (4/\pi\hbar) \text{ photons/cm}^2\text{-sec} \quad \text{(E-XXVI)}$$

from which it follows that

$$\langle F \rangle^3 = 7.08 \times 10^{99} \frac{P^3}{\nu^3\theta^6\Gamma^6} \text{ photons}^3/\text{cm}^6\text{-sec}^3 \quad \text{(E-XXVII)}$$

where $\nu = \omega/2\pi$.

Finally $\langle F \rangle^3$ may be replaced by $(1/h)\langle F^3 \rangle$ where

h is a correction factor dependent upon the spatial profile of the flux. While the relative nature of the experiment renders h unimportant, it is, in principle, obtained from the divergence measurement in Section VI B.

G. Conclusion

Eq. (E-VI) expresses δ_3 in terms of N, $\langle v \rangle$, J(x,y), d, n and F. Of these seven quantities, five are not directly measured but are, rather, obtained through the measurement of other experimental parameters (the measurement of N is obtained from the gain of the electron multiplier). It has been the purpose of this chapter to rewrite Eq. (E-VI) so that we obtain an expression for δ_3 as a function only of directly measured quantities. Combining Eqs. (E-VI), (E-IX), (E-X), (E-XIV), (E-XV), (E-XIX), (E-XLIV), and (E-XXVII), and inserting into the result those values of the parameters which remain constant throughout the experiment, we can finally write

$$\delta_3 = 2.44 \times 10^{-117} \frac{N(T/M)^{\frac{1}{2}} \nu^3 \theta^4 \Gamma^4}{nI_o \int \langle F \rangle dt} \text{ cm}^6\text{-sec}^2 \quad \text{(E-XXVIII)}$$

MEASUREMENTS

The actual measurements were performed by cross-firing the atomic beam with the laser, and recording the trace of electron multiplier and photodiode output signals. The time-evolution of the photodiode signal is most important, because of the non-linearity of the process and the lack of pulse-to-pulse reproducibility for the laser. The overall rise time of the photodiode and its associate circuitry was about 1 nsec, quite sufficient to record the variation in the experiment. (This includes the 1 GHz traveling wave oscilloscope, which we used to record the photodiode output signal.) From the photographed trace of the traveling wave CRT, we obtain the laser power P as a function of time. From P(t) we can obtain $P^N(t)$, where N is the order of the process.

In the experiment, a quarter wave plate was rotated to produce circular and linear polarized light as desired. (A random sequence was used to eliminate the effect of any periodic variation in the laser output.) Both states of circularly polarized light were examined, and, as expected, showed no measurable difference. A sizeable difference between linearly and circularly polarized was observed. This discovery was the outstanding achievement of the project.

The experimental results are as follows.

Cesium: $R_3 = 1.71 \pm .33$, at ruby laser frequency; $R_2 = 1.28 \pm .21$, at ruby second harmonic.

Potassium: $R_3 = 0.904 \pm .229$, at ruby laser frequency.

($R_N = \delta_N$(circularly polarized light)$/\delta_N$(linearly polarized light).)

DETAILED CALCULATION

As we indicated earlier, detailed calculations for the three quantum ionization of cesium have been performed. Similar results for the two-quantum process have also been completed. In this section, we will outline the procedures by which these calculations have been done.

We make use of a model in which the cesium atoms are treated in a single-electron approximation. For this purpose, the valence electron moves under the influence of a potential which accurately reproduces the ground, lowest p-, and lowest d-state energies. (For $L \neq 0$, the potential reproduces the weighted average of the doublet energy.) The potential behaves like -Z/r for small r, and like -1/r for r going to infinity. The effect of the 54 core electrons is ignored, except insofar as they contribute to the potential for the valence electron. For the two quantum process, we must solve the differential equation

$$\left[-\frac{d^2}{dr^2} + V(r) + \frac{L_1(L_1+1)}{r^2} - \mathcal{E}_0 - \hbar\omega\right]\phi_1 = r\mathcal{M}_0 \quad . \qquad \text{(C-I)}$$

The unperturbed wave function $\Psi_0 = \mathcal{M}_0(r)Y_0^0(\Omega)$.

The final state partial wave function is $\Psi_F = \frac{\mathcal{M}_F^{(2)}(r)}{r} Y_{L_F, M_F}(\Omega)$.

For the three quantum process we solve

$$\left[-\frac{d^2}{dr^2} + V(r) + \frac{L_1(L_1+1)}{r^2} - \mathcal{E}_0 - \hbar\omega\right]\phi_1 = r\mathcal{M}_0 , \qquad \text{(C-II)}$$

$$\left[-\frac{d^2}{dr^2} + V(r) + \frac{L_2(L_2+1)}{r^2} - \mathcal{E}_0 - 2\hbar\omega\right]\phi_2 = r\mathcal{M}_F^{(2)}(r)$$

Unlike previous work, we solved the differential equations by means

of numerical forms of the Green's function. The Green's function satisfies the inhomogeneous differential equation with the delta-function inhomogeneity

$$\left[-\frac{d^2}{dr^2} + \frac{2\lambda(\lambda+1)}{r^2} + V(r) - \mathcal{E}_0 + \hbar\omega'\right] G_\lambda^{\omega'}(r, r') = \delta(r - r') \qquad \text{(C-III)}$$

The solution of the desired inhomogeneous equation is obtained by the quadratures

$$\phi_1 = \int_0^\infty G_{L_1}^{\omega}(r, r')\, r'\, u_0(r')\, dr',$$

$$\phi_2 = \sum_0^\infty G_{L_2}^{2\omega}(r, r')\, r'\, u_F^{(L_F)}(r')\, dr'.$$

$$G_\lambda^{\omega'} = A\, u(r_<)\, v(r_>), \quad \left[-\frac{d^2}{dr^2} + \frac{2\lambda(\lambda+1)}{r^2} + V(r) - \mathcal{E}_0 - \hbar\omega\right] N$$

$$= 0. \qquad \text{(C-IV)}$$

In general, $E_0 + \hbar\omega$, etc, are not eigenvalues of the differential equation, so that the solutions, u(r), v(r), which are regular for small and large values of r, are not the same function, i.e., u goes to infinity for r going to infinity, and v goes to infinity (or to a non-zero value for L=0) as r goes to zero. The Green's function is then of the form $Au(r_<)\, v(r_>)$, where the constant A is chosen to make the coefficient of the delta function on the left side of the top

equation equal to unity, in accord with the right side.

The functions u, v are obtained numerically. We assume the asymptotic expansion for v at large values of r that is appropriate for a Coulomb potential. This is integrated inward. We take a power series for u near the origin, and then integrate outward. In general, u will diverge exponentially at large r, and v goes as r^{-L} at small r. Quadratures are obtained by Simpson's rule, and the differential equations for u and v are solved by Numerov's method, since the first derivative has a vanishing coefficient.

Calculated results for the two and three quantum transition rates in cesium are tabulated below. Our result for the ratio of the linearly polarized transition rate to the circularly polarized transition rate is in good agreement with experiment, as is the second harmonic two-quantum result. Lambropoulos[6] has also obtained good agreement in the two quantum case, although he used much simpler (hydrogenic 2s) wave functions. This seeming success of this very crude approximation can be understood as follows. We see that our table gives practically a constant relative transition probability over a substantial frequency range. (The relative transition probability measures the ratio of the p to s and p to d radial integrals.) As long as resonances are not important, we may approximate the intermediate summation by the same one or two terms, which, in this case, happen to yield intermediate to final state radial integrals of the same relative magnitudes in hydrogen and cesium. The situation changes as a state goes through a resonance, especially where we must consider both the resonant and non-resonant terms as interfering. In short, it appears that the relative two photon rate tends systematically to be near 1.3, but that wide divergences occur in the vicinity of intermediate state near-resonances.

TWO-PHOTON IONIZATION OF CESIUM (THEORY)

Photon Energy (Rydberg)	Linear Transition Rate (cm^4-sec)	Relative trans. rate (Circular/linear)
.156	9.73 x10-49	1.33
.161	4.56 "	1.33
.165	3.13 "	1.33
.170	2.15 "	1.34
.175	1.43 "	1.34
.179	9.06 x 10^{-50}	1.35
.184	5.06 "	1.36
.189	2.00 "	1.40
.193	1.11 x10-51	1.47
.198	3.27 x10-50	1.19
.203	1.54 x10-48	1.28
.207	1.39 "	1.30
.212	2.75 x10-49	1.32
.217	1.25 "	1.33
.221	6.82 x10-50	1.34
.226	3.58 "	1.35
.231	1.05 "	1.36
.235	9.64 "	1.41
.240	1.58 x10-49	1.39
.245	8.83 x10-50	1.31
.249	2.37 x10-49	0.906
.254	3.44 x 10-48	0.220
.259	6.02 x 10-49	0.0130
.264	2.95 x 10-48	1.39
.268	7.97 "	0.562
.273	1.63 "	0.577
.278	2.23 "	0.410
.282	1.55 "	0.157

THREE-PHOTON IONIZATION OF CESIUM (THEORY)

Photon Energy (Rydberg)	Linear Trangition Rate (cm^6-sec^2)	Relative Transition Rate (Circular/linear)
0.100	2.18 x 10^{-76}	0.030
0.102	5.60 x 10^{-77}	2.20
0.103	1.66 x 10^{-76}	0.817
0.105	1.26 x 10^{-75}	2.50
0.107	2.20 x 10^{-74}	2.37
0.108	1.98 x 10^{-74}	2.34
0.110	5.03 x 10^{-76}	2.10
0.111	7.69 x 10^{-77}	1.12
0.113	5.19 x 10^{-78}	0.868
0.114	2.19 x 10^{-79}	0.520
0.116	5.42 x 10^{-79}	0.796
0.118	2.32 x 10^{-76}	0.065
0.119	4.94 x 10^{-77}	2.47
0.121	1.94 x 10^{-77}	2.41
0.122	5.33 x 10^{-78}	0.088
0.124	1.05 x 10^{-77}	0.498
0.126	9.79 x 10^{-77}	0.281
0.127	1.33 x 10^{-75}	1.59
0.129	2.05 x 10^{-77}	0.952
0.130	9.70 x 10^{-78}	0.016
0.132	2.40 x 10^{-76}	2.03
0.134	2.39 x 10^{-77}	0.861
0.135	2.33 x 10^{-77}	1.34
0.137	2.38 x 10^{-79}	2.49
0.138	1.45 x 10^{-77}	0.497
0.140	1.38 x 10^{-77}	1.14
0.142	3.38 x 10^{-78}	2.28

Personnel

Principal Investigator: Prof. Edward J. Robinson

Scientific Personnel:

Robert A. Fox, Instructor in Physics

Robert. M. Kogan, N.S.F. Fellow

Geoffrey T. Burnham, Research Assistant

Secretary:

Blanche Hoffenberg

REFERENCES

1. M. Goeppert-Mayer, Naturwissenschaften, 17 932 (1929); Ann. Phys., 9 273 (1931).

2. R. A. Fox, R. M. Kogan and E. J. Robinson, Phys. Rev. Letters 26, 1416 (1971).

3. H. B. Bebb and A. Gold, Phys. Rev. 143, 1 (1966).

4. P. Hammerling, Royal Society Conference on Optical Masers (1962).

5. H. B. Bebb, Phys. Rev 149, 25 (1966); Phys. Rev 153 23 (1967).

6. P. Lambropoulos, Phys. Rev. Letters 29, 453 (1972).